Ann. Geophysicae 16, 986–996 (1998) © EGS – Springer-Verlag 1998

Annales Geophysicae

Trends in the ionospheric E and F regions over Europe

J. Bremer

Institut für Atmosphärenphysik, Schloßstr. 6, D-18225 Kühlungsborn, Germany

Received: 12 November 1997 / Revised: 9 March 1998 / Accepted: 11 March 1998

Abstract. Continuous observations in the ionospheric E and F regions have been regularly carried out since the fifties of this century at many ionosonde stations. Using these data from 31 European stations long-term trends have been derived for different parameters of the ionospheric E layer (h' E, foE), F1 layer (foF1) and F2 layer (hmF2, foF2). The detected trends in the E and F1 layers (lowering of the E region height h'E; increase of the peak electron densities of the E and F1 layers, foE and foF1) are in qualitative agreement with model predictions of an increasing atmospheric greenhouse effect. In the F2 region, however, the results are more complex. Whereas in the European region west of 30° E negative trends in hmF2 (peak height of the F2 layer) and in the peak electron density (foF2) have been found, in the eastern part of Europe (east of 30° E) positive trends dominate in both parameters. These marked longitudinal differences cannot be explained by an increasing greenhouse effect only, here probably dynamical effects in the F2 layer seem to play an essential role.

Key words Atmospheric composition and structure (Pressure, density and temperature) · Ionosphere (Mid-latitude ionosphere) · Radio science (Ionospheric propagation).

1 Introduction

Based on the results by Roble and Dickinson (1989) with a globally averaged model of the coupled meso-, thermo- and ionosphere, Rishbeth (1990) predicted a lowering of E and F2 peak heights (hmE, hmF2) by about 2.5 km and 15–20 km if the atmospheric CO_2 and CH_4 content is doubled. The expected changes in the E and F2 peak electron densities should be small. In a more recent paper Rishbeth and Roble (1992) investigated the atmospheric greenhouse effect for December solstice conditions with the 3-dimensional TIGCM (thermosphere/ionosphere general circulation model) developed at the National Center for Atmospheric Research, Boulder. Assuming again a doubling of the greenhouse gases, a lowering of hmF2 by 10–20 km was derived whereas the electron density at the peak height of the F2 layer and above decreases (foF2 decreases up to 0.5 MHz) but below the F2 peak the electron density increases (including F1 and E regions).

Using the data of individual ionosonde stations Bremer (1992) with observations from Juliusruh and Poitiers and more recently Ulich and Turunen (1997a) with data from Sodankylä found a significant lowering in hmF2 during the last 40 years. Recent investigations by Bremer (1996, 1997a,b) and by Ulich and Turunen (1997b) gave, however, some hints that the trends in the F2 region are not so uniform as expected. Therefore, in this study the data of all available European ionosonde stations are considered to provide more reliable results about the thermospheric trends in dependence on latitude, longitude and altitude. In these analyses characteristic parameters of the F2 layer (hmF2, foF2), of the F1 layer (foF1) and of the E layer (h'E, foE) have been used. The large amount of data necessary for these investigations were extracted from different CD-ROMs of the National Geophysical Data Center (NGDC), Boulder, Colorado, USA and from the WDC-C at the Rutherford Appleton Laboratory (RAL), Chilton, Didcot, UK.

2 Experimental data and data analysis

Data from 31 European ionosonde stations (5° W – 70° E, 35° N –70° N) have been used for trend analyses. In Table 1 these stations are presented in dependence on latitude. The trend coefficients given will be discussed later in Sects. 3 and 4.

In the trend analyses we used only monthly median values of the different ionosonde parameters. It is well-known that these parameters depend markedly on solar

Table 1. Ionosonde stations with geographic coordinates (latitude and longitude) and trend coeffcients b derived for different characteristic parameters of the ionospheric E, $F1$ and $F2$ regions

Station	Latitude	Longitude	$b(foE)$	$b(h'E)$	$b(foF1)$	$b(hmF2)$	$b(foF2)$
Loparskaya	68.0	33.0	−0.0008			−0.2674[a]	0.0023
Kiruna	67.8	20.4	0.0028[a]	−0.0099		0.0101	0.0028
Sodankylä	67.4	26.6				−0.2153[a]	−0.0160[a]
Salekhard	66.5	66.5	−0.0014[a]			0.0804	−0.0032
Arkhangelsk	64.6	40.5	0.0013			0.4228[a]	0.0017
Lycksele	64.6	18.8	0.0053[a]			−0.0037	0.0016
Nurmijärvi	60.5	24.6				−0.4600[a]	−0.0290[a]
Leningrad	60.0	30.7	0.0004			−0.1986[a]	−0.0008
Uppsala	59.8	17.6	0.0026[a]	−0.0466	−0.0006	−0.1475	−0 0028
Sverdlovsk	56.4	58.6	0.0046[a]			0.4394[a]	−0.0002
Gorky	56.1	44.3	0.0007			0.1225	−0.0031
Moscow	55.5	37.3	0.0047[a]			0.8444[a]	0.0029
Kaliningrad	54.7	20.6	0.0002			0.1606	−0.0028
Juliusruh	54.6	13.4	−0.0002	−0.2773[a]	0.0000	−0.1850[a]	−0.0026
Slough	51.5	−0.6	0.0003	0.3274[a]	0.0002	0.2853[a]	−0.0014
Kiev	50.5	30.5	0.0010		0.0015	0.1923[a]	0.0012
Dourbes	50.1	4.6	0.0017[a]	−0.0935[a]	0.0112[a]	−0.0191	0.0053
Pruhonice	50.0	14.6					−0.0107[a]
Lannion	48.5	−3.3	0.0029[a]		0.0059[a]	0.3800	0.0083
Freiburg	48.1	7.6		−0.1687[a]		−0.4551[a]	−0.0013
Rostov	47.2	39.7	0.0009		0.0018[a]	0.4183[a]	0.0049
Bekescaba	46.7	21.2				−0.4392[a]	−0.0063
Poitiers	46.6	0.3	0.0045[a]		0.0028[a]	−0.4208[a]	0.0074[a]
Novokazalinsk	45.5	62.1	0.0004		−0.0008	0.0521	−0.0056
Beograd	44.8	20.5		−0.0230		−0.3987[a]	−0.0070
Sofia	42.7	23.4	0.0024	−0.3282[a]	0.0018		−0.0023
Rome	41.8	12.5	0.0018	−0.4052[a]	−0.0057[a]	−0.2566[a]	0.0088[a]
Tbilisi	41.7	44.8	0.0056[a]			−0.0310	0.0027
Tashkent	41.3	69.6	0.0005			0.1368	0.0022
Ashkhabad	37.9	58.3	0.0012		0.0006	0.7329[a]	0.0015
Gibilmanna	37.6	14.0	0.0044[a]	0.2136			−0.0145

[a]Indicates significant trends (> 90%)

and geomagnetic activity. To detect relatively small trends in the ionospheric parameters it is therefore necessary to remove these strong influences, e. g. by a simple regression analysis. We calculated for the experimental data X ($X = hmF2, foF2, foF1, h'E$ or foE) for each complete hour (0–23 UT) and each month the following regression equations

$$X_{th} = A + B\,R + C\,Ap. \tag{1}$$

Here R is the solar sunspot number and Ap the planetary geomagnetic activity index. Instead of R also the solar flux data F 10.7 can be used to characterize the solar activity, the results of the trend analysis do not depend on this choice. Using the results of the regression analysis after Eq. (1) we calculated the deviations ΔX of the experimental hourly data $X_{\exp}$ from these theoretical values X_{th}

$$\Delta X = X_{\exp} - X_{th}. \tag{2}$$

With these ΔX values linear trends can be estimated according to

$$\Delta X = a + b \text{ year}. \tag{3}$$

In this way it is possible to derive trend parameters b for each hour and each month. In this work the hourly and monthly ΔX values have normally been averaged to calculate more reliable yearly ΔX values and yearly trends after Eq (3).

The test of the significance of the trend parameter b can be made with Fisher's F parameter

$$F = r^2(N-2)/(1-r^2). \tag{4}$$

Here r is the correlation coefficient between ΔX and year after Eq. (3), and N is the number of years used in the analysis. The significance levels to be exceeded by the F parameter after Eq. (4) can be found in Taubenheim (1969). Significant trends with a confidence level of more than 90% are maked in Table 1 or with solid symbols in Figs. 1–6.

3 Results

3.1 F2 region

The peak height of the F2 layer ($hmF2$) and the electron density at this height ($foF2$) are used in the trend investigations of the F2 region. The value of $hmF2$ was derived from observed monthly $M(3000)F2$ values using the well-known formula of Shimazaki (1955)

$$hmF2 = 1490/M(3000)F2 - 176. \tag{5}$$

As shown by Bremer (1992) the choice of this simple formula is not critical for the derived trends, the trends are nearly identical if the more accurate formula of Bilitza *et al.* (1979) is used for the estimation of *hm*F2.

In Fig. 1 the results of the trend analysis for *hm*F2 values are separately presented for European stations at longitudes less than 30° E in the upper part of this figure and at longitudes greater than 30° E in the lower part. In both cases the trends are ordered in dependence on latitude, shown in brackets below the name of the station. If the linear trends are significant with more than 90% the yearly data ΔhmF2 are presented by solid dots, if the significance level is smaller than 90% open circles have been used. The numerical values of the derived trend coefficients can be found in Table 1. Whereas the trends do not show a dependence on latitude in the latitudinal belt investigated between 35° N and 70° N, there are marked differences between the two longitudinal regions west and east of 30° E. In the part west of 30° E 11 of 15 trends are negative, from 9 significant trends are even 8 negative. In the eastern part of Europe (east of 30° E) the results are quite opposite. Eleven of 13 trends including 7 of 8 significant trends are positive. This marked difference can also be seen in Fig. 2 where the *hm*F2 trend parameters are shown in relation to longitude. The two straight lines mark the median values of the individual trends in the two longitudinal zones: −0.18 km/y and 0.19 km\y. The corresponding mean values for both regions which slightly deviate from the median values shown in Fig. 2 are significantly different with more than 99% as can easily be shown by a t-test (Taubenheim 1969).

The trends of *fo*F2 are presented in Fig. 3 in a similar way as for *hm*F2 in Fig. 1. Also the *fo*F2 trends do not markedly depend on latitude. But there seems to exist again a difference between the two longitudinal regions west or east of 30° E. The median values of the *fo*F2 trends are: −0.0024 MHz/y for the western part (stations in the upper part of Fig. 3) and 0.0015 MHz/year for the eastern region (lower part of Fig. 3). The scatter of the values is however markedly higher than for the corresponding *hm*F2 trends presented already. Therefore, the concept that the mean trends of *fo*F2 in both regions are different could be shown with only a low significance level of about 84%. This behaviour can also be supported by the fact that in the western part 12 of 18 trends are negative (but from 6 significant trends are 3 negative and 3 positive) whereas in the eastern part 8 of 13 trends are positive (here no significant trends could be discerned!).

As a summary it can be stated that in the F2 layer above the European region in *hm*F2 and *fo*F2 trends no marked differences in dependence on latitude could be found but clear differences between the trends in the longitudinal regions west and east of about 30° E. In the western part the trends are mainly negative and in the eastern part dominantly positive. The correlation coefficient between the *hm*F2 and *fo*F2 trend values is due to the strong scatter of the individual trends (especially in the *fo*F2 trends) only $r = 0.38$. Nevertheless this value is after the *t*-test (Taubenheim, 1969) with 95% significance).

3.2 F1 region

The peak electron density of the F1 layer, *fo*F1, has been used for a trend analysis at F1 region heights near 170–180 km. Unfortunately only values of 12 stations were available, 4 stations for the region east of 30° E and 8 stations in the western part of Europe. In Fig. 4 the trend results are therefore presented only in their dependence on latitude and not subdivided into different longitudinal regions. The trends are in most cases positive (9 of 12 trends including 4 of 5 significant trends) with a median value 0.001 MHz/year. In agreement with the results in the F2 region in the F1 layer the trends do not markedly depend on the latitude, but in contrast to the F2 layer in the F1 layer no marked differences could be found also for different longitudinal regions. At longitudes west of 30° E 6 of 8 stations have positive trends, and at longitudes east of 30° E 3 of 4 trends are positive.

3.3 E region

The E region reflection height *h'*E and the peak electron density *fo*E have been used for trend analyses at E region heights (110–120 km). In Fig. 5 the results for *h'*E are presented. Unfortunately only observations at 10 stations are available, and all of them are from the western part of Europe. From most of measurements negative trends were derived (8 of 10 including 5 of 6 significant trends) with a median value −0.07 km/year. Also here the trends do not show a marked dependence on latitude.

In Fig. 6 the *fo*E trends for 25 European stations are shown, separated again for two longitudinal regions west (upper part) and east of 30° E (lower part). The trends are relatively uniform, 22 of 25 trends (including 10 of 11 significant trends) are positive. The median trend value is 0.0013 MHz/year. Marked longitudinal and latitudinal dependencies could not be found in the European E region investigated.

4 Discussion

As the ionospheric plasma parameters are markedly controlled by the solar activity it is necessary to remove this part carefully if derivation of long-term trends are required which are normally more than one order of magnitude smaller than the solar induced variations. In this study a linear dependence of the plasma parameters on solar as well as geomagnetic activity is adopted to describe the solar influence. This model is very similar to a model used by Kane (1992) to get a better description of the hysteresis effect in *fo*F2 observations. Kane (1992)

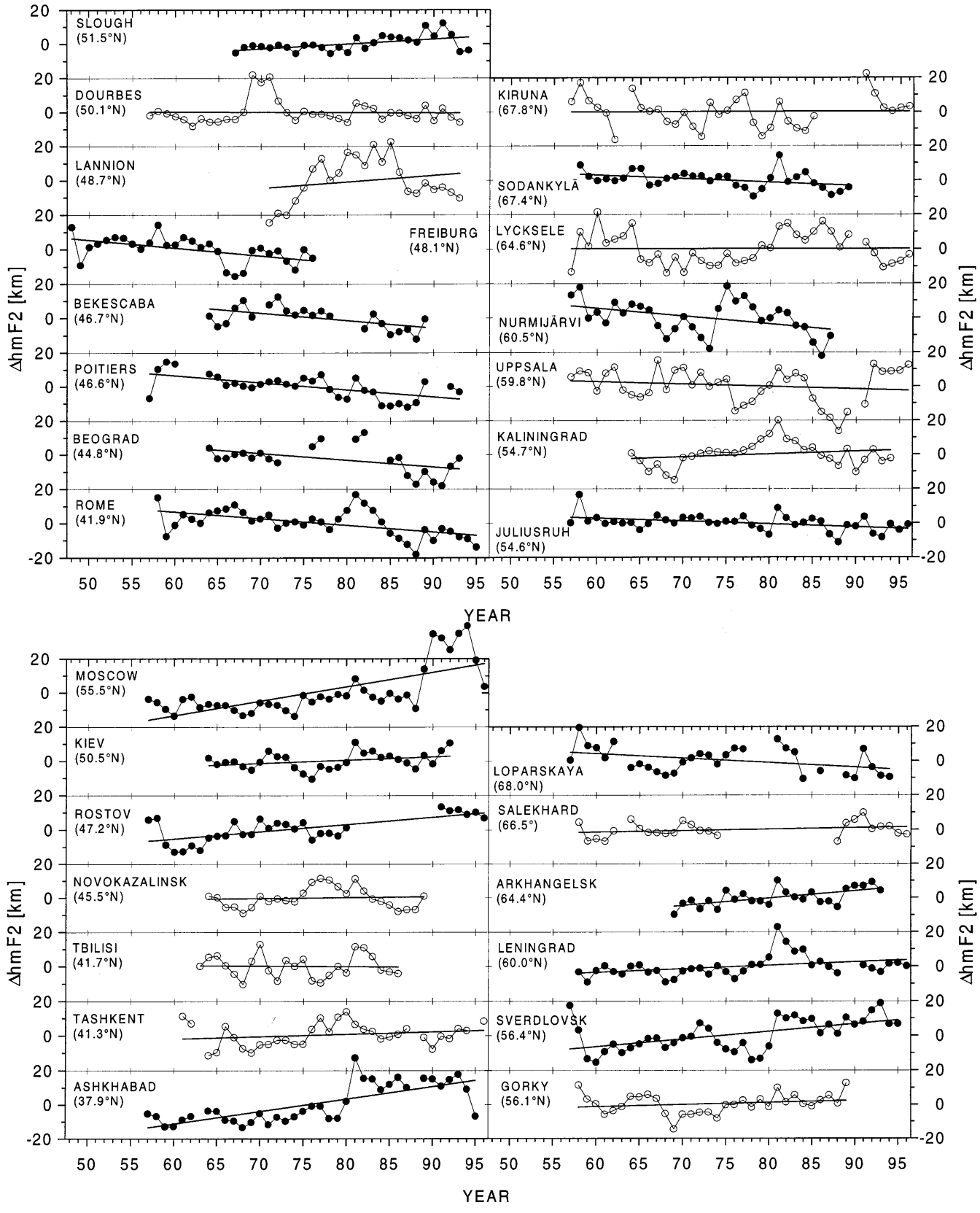

Fig. 1. Yearly trends of Δ*hm*F2 after elimination of the solar and geomagnetic influences for European stations at longitudes west of 30°E (*upper part*) and at longitudes east of 30°E (*lower part*). Significant trends (>90%) are marked by *solid dots*

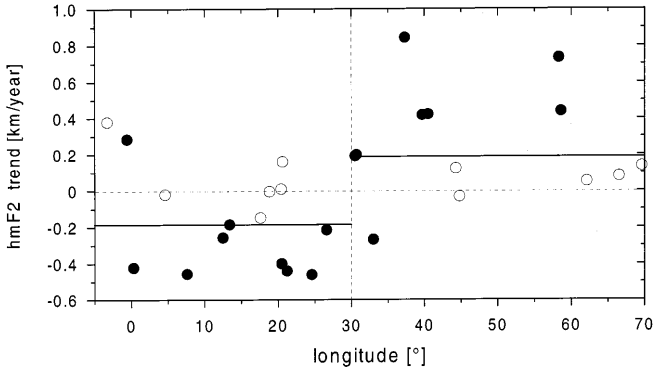

Fig. 2. *hm*F2 trend coefficients dependent on longitude. Significant trends are marked by *solid dots*. The *solid lines* represent the median values of all individual trends in the regions west or east of 30°E

only used the solar 10.7 cm radio flux (F10.7) instead of the solar sunspot number R but also the geomagnetic Ap index. After Kouris *et al.* (1994) *fo*F2 is slightly better correlated with solar activity if a quadratic relation is assumed ($f(R, R^2) = a + bR + cR^2$). This effect can be seen in Fig. 7 where the monthly mean noon values (12 LT) of *fo*F2, *hm*F2, *fo*F1, *fo*E, and *h'*E from observations at Juliusruh between 1957 and 1996 are presented showing their dependence on solar activity. The data for January (crosses) and July (solid circles) are shown together with the linearly (complete lines) and quadratically fitted curves (dashed). The differences between the linear and quadratic approximations are often very small but sometimes remarkable (e.g. *hm*F2 in July). The quality of the different approximations of the solar-induced variations can be tested by correlation coefficients between the observed data with the different model results of these data. In Fig. 8 these correlation coefficients are presented for *fo*F2 and *hm*F2 data from Juliusruh for January and July dependent on local time. All correlation coefficients are highly significant, also for the parameters *fo*F1 and *fo*E (not shown here), although the correlation of *h'*E with solar activity is markedly smaller. The differences between the correlation coefficients for the same ionospheric parameter are very small. In most cases the correlation with the linear $f(R)$ model (open circles in Fig. 8) is slightly smaller and the best correlations have been found sometimes for the $f(R, Ap)$ values (crosses) and sometimes for the $f(R, R^2)$ values (solid circles). In Fig. 9 the trends in *fo*F2 and *hm*F2 for Juliusruh are presented using different models to remove the solar-induced variation. Here all data (all 24 h of all 12 months) have been used as in Figs. 1–6. The general agreement of the three different curves of the $\Delta foF2$ and $\Delta hmF2$ values in Fig. 9 is very good, indicating that the derived trends do not depend greatly on the model used to eliminate the solar-induced variation. In detail small differences may occur in the individual data, the general behaviour, however, is little influenced by the choice of the model. In particular the $f(R, R2)$ and the $f(R, Ap)$ models give very similar results.

Independent of the model used the removal of the solar-induced variation requires a long data series. Therefore in this study nearly all data series investigated are longer than 20 y with only very few exceptions, as can be seen in Figs. 1–6.

The model calculations for an atmospheric greenhouse effect are normally carried out for a doubling of the greenhouse gases CO_2 and CH_4. To compare these theoretical results with our experimental trend data it is necessary to take into account the real changes of these gases during the last 40 y, corresponding to the main interval of ionosonde observations which has been analysed here. After the recent IPCC report (Houghton *et al.,* 1996) and Brasseur and de Rudder (1987) the atmospheric content of these gases has increased during the last 40 y for CO_2 by about 15%, CH_4 by about 44%, N_2O by about 7% and for the CFCs and HCFCs partly by essentially higher rates (yearly increases between 0.5%). Taking into account the different amounts of these greenhouse gases, for the total direct radiative forcing, after Houghton *et al.* (1996) an effective increase of the greenhouse gases of about 20% can be assumed for the last 40 y.

After the model calculations of Rishbeth (1990) and Rishbeth and Roble (1992) the F2 peak height *hm*F2 should be lowered by about 10–20 km if the greenhouse gases are doubled, corresponding to a lowering of about 2–4 km for the last 40 y. The median experimental trends derived in this study however, give a lowering of 7.2 km (at longitudes west of 30° E) or an increase of 7.6 km (at longitudes east of 30° E) for the last 40 y. Whereas the experimental lowering of *hm*F2 in the western part of Europe is only slightly stronger than the theoretically expected result, in the eastern part even the direction between predicted and observed trend values is contrary. Such a behavior of regional differences in the *hm*F2 trends has also been found by Ulich and Turunen (1997b) using data from ionosonde stations all around the world. It is difficult to decide if technical changes of the equipment or changes in the evaluating algorithm could be responsible for the considerable differences especially for the unexpected positive trends in the eastern part of Europe. Therefore, for three stations of this region the *hm*F2 trends are shown in Fig. 10 once again. Indeed there seem to be some discontinuities in the trends (marked by dotted vertical lines) which could be caused by technical changes, but nevertheless there remain large parts of the observations with positive trends. Therefore, the trends of individual stations may be partly influenced by technical changes, but it seems to be impossible to argue that the positive trends in the eastern part of Europe and in other regions of the world as found by Ulich and Turunen (1997) are only caused by artificial changes.

Similar differences to those for *hm*F2 trends were also detected in the *fo*F2 trends in Fig. 3. In the western part of Europe we detected a mean *fo*F2 decrease during the last 40 y of about 0.1 MHz which is in relatively good agreement with the results of Rishbeth and Roble (1992) who predicted a lowering up to about 0.5 MHz for a doubling of the greenhouse gases. But in the eastern part

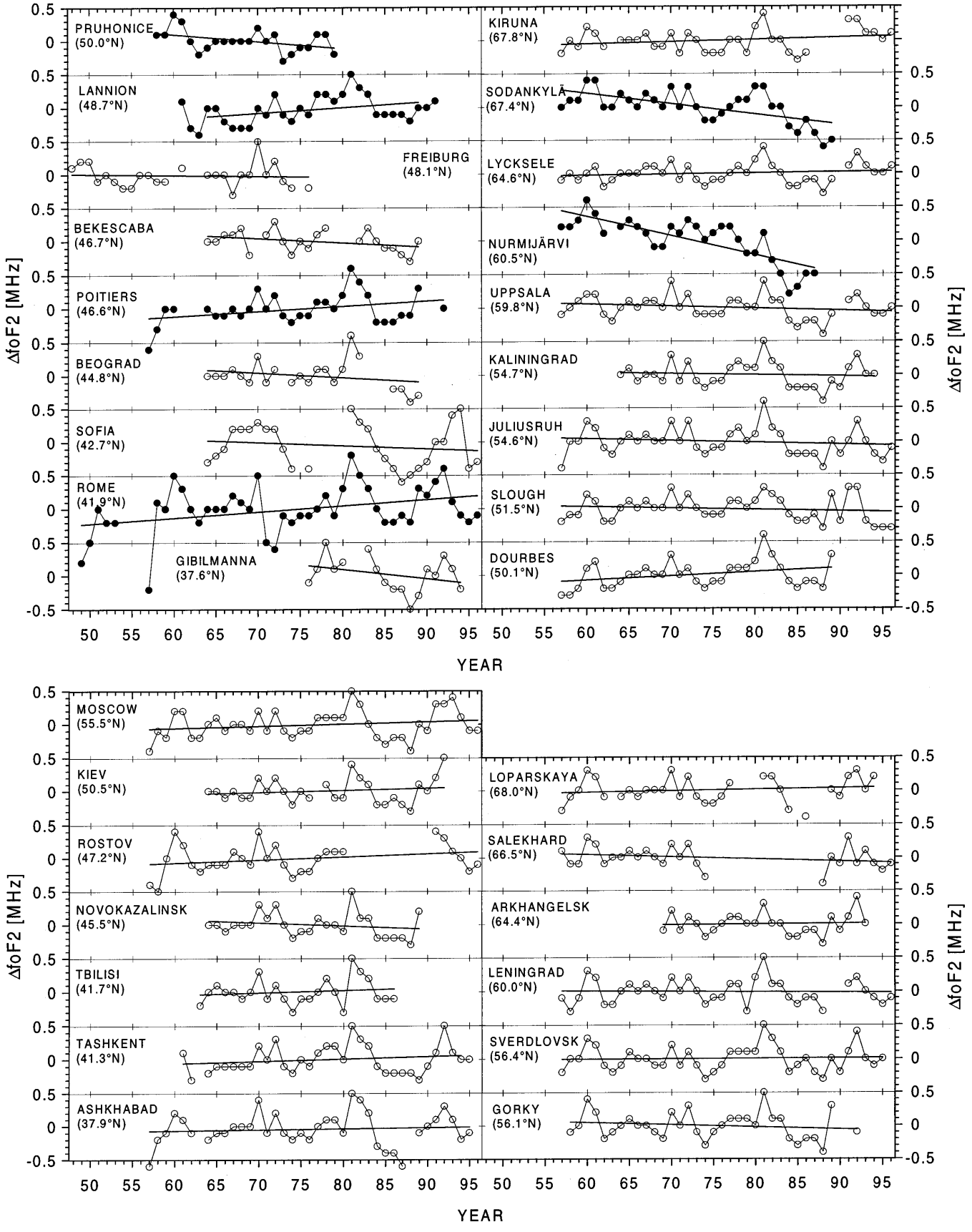

Fig. 3. Same as Fig. 1, but for Δ*fo*F2 values

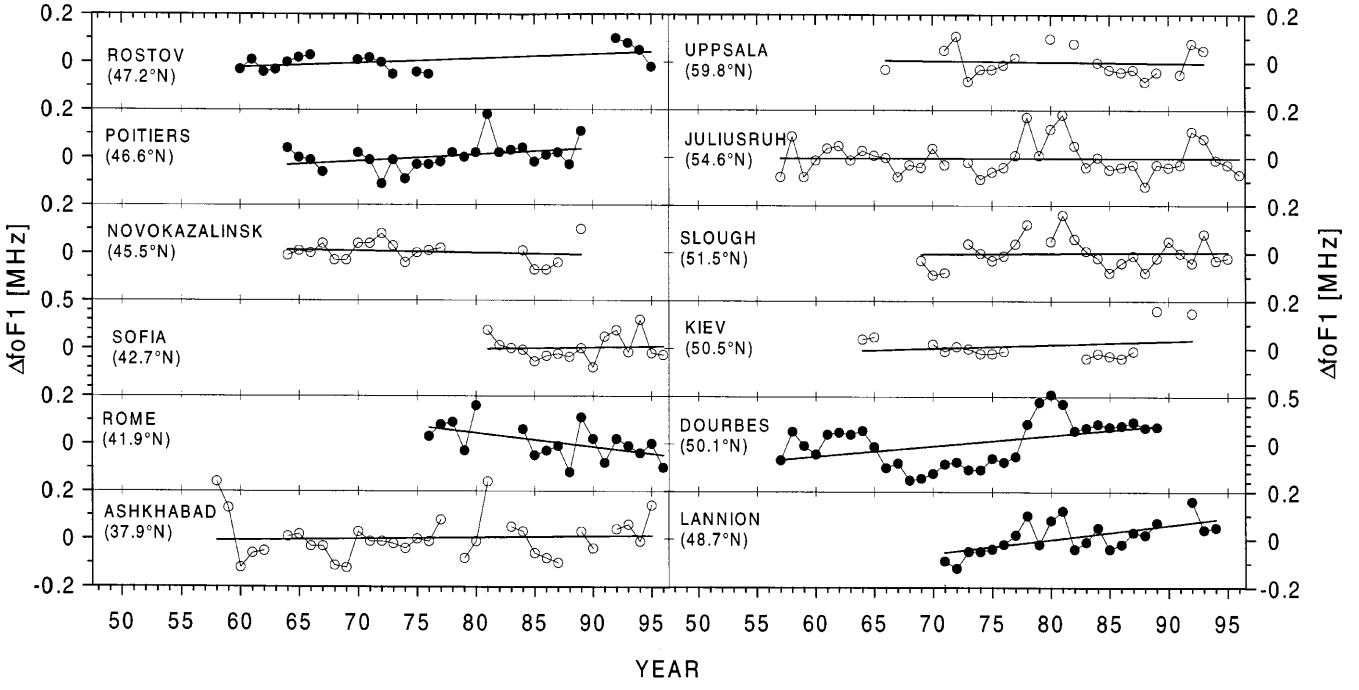

Fig. 4. Same as Fig. 1, but for Δ*fo*F1 values and not subdivided into different longitudinal regions

of Europe an increase of about 0.06 MHz was detected in contrast to the predicted reduction of Rishbeth and Roble (1992). In general the differences between the *fo*F2 trends in the western and eastern part of Europe qualitatively agree with the differences in the *hm*F2 trends, however the differences in the *hm*F2 trends seem to be more pronounced. The reason for these longitudinal differences are not yet known, but they are probably caused by the complex dynamics of the F2 region. The *hm*F2 and *fo*F2 maps derived with the TIGCM by Rishbeth and Roble (1992) contain structures which could be connected with different regional trends of these F2 region parameters. However detailed experimental and theoretical investigations are necessary in the future to reach a better understanding of trends in the F2 region dependent on latitude and longitude.

At lower heights (F1 and E regions) where dynamical processes are not so dominant as in the F2 layer latitudinal as well as longitudinal differences could not be detected. Using the median *fo*F1 trend of 0.001 MHz/year a mean *fo*F1 increase of 0.04 MHz during the last 40 y was derived from the experimental results. Rishbeth and Roble (1992) derived, with their model calculations, an increase in the electron density near the peak height of the F1 layer between 5% and 50%, with a median value

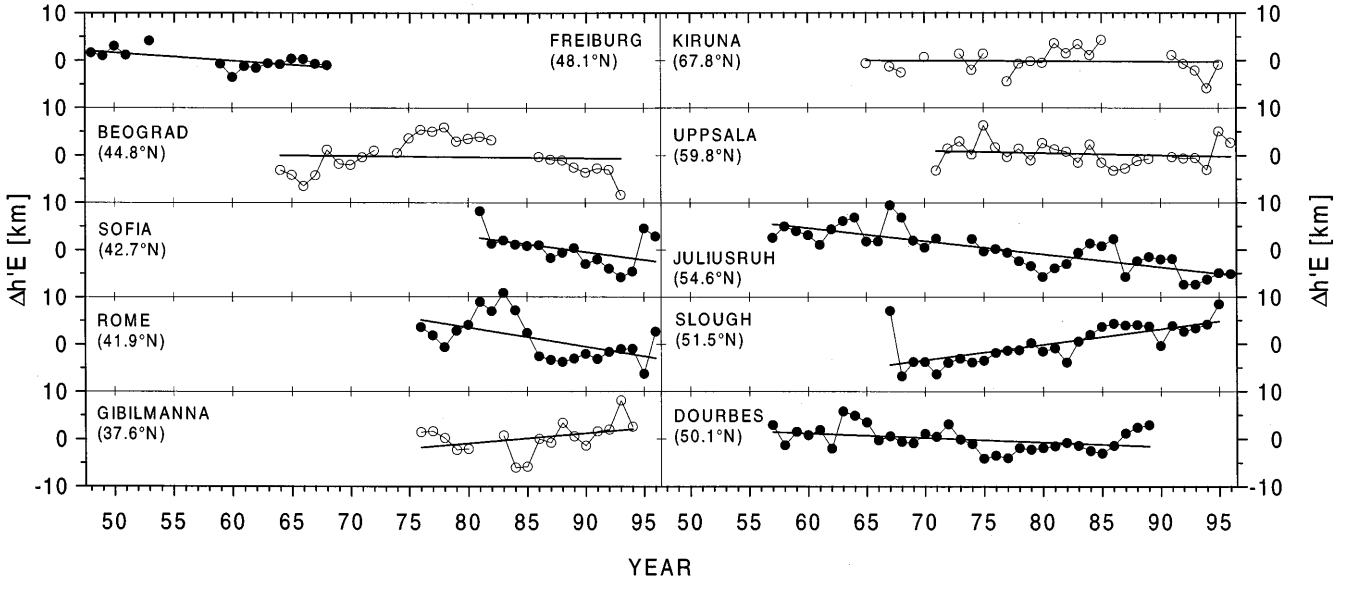

Fig. 5. Same as Fig. 1, but for Δ*h*'E values and not subdivided into different longitudinal regions

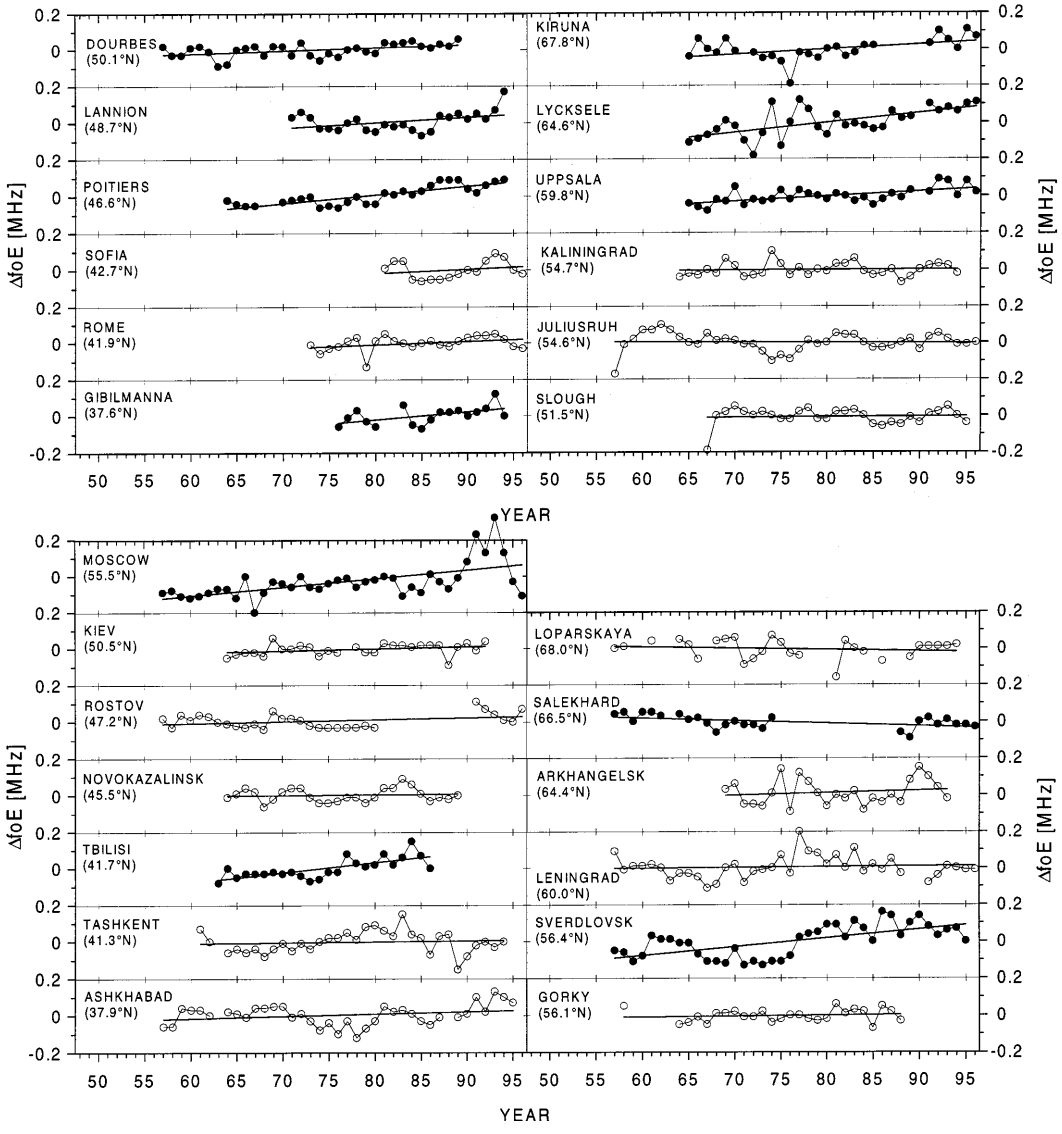

Fig. 6. Same as Fig. 1, but for Δ*fo*E values

near 15% corresponding to a mean increase in *fo*F1 up to about 8% for a doubling of the greenhouse gases. For typical *fo*F1 values of 4–6 MHz an *fo*F1 increase of 0.3–0.5 MHz (or an increase of about 0.06–0.1 MHz for the last 40 y) can be expected from the modelling results. The agreement with the mean experimental trend value is quite reasonable, the median experimental trend is only smaller by a factor of about 2.

In the E region two parameters have been used for trend investigations, *h*′E and *fo*E (see Figs. 5 and 6). With the median trend value of -0.07 km/y we get a lowering of the E region by about 2.8 km during the last 40 y which is in the same order as predicted by Rishbeth (1990) for a doubling of the greenhouse gases. Therefore, the experimental value is higher than the predicted value by about a factor of 5. Using the mean *fo*E trend of 0.0013 MHz/year a *fo*E increase of about 0.05 MHz was observed during the last 40 y. After the model calculations of Rishbeth and Roble (1992) an increase of the electron density at E region heights of about 5% (corresponding to an increase in *fo*E by about 2.5%) is predicted for a doubling of the greenhouse gases. For typical *fo*E values of 2–3 MHz an *fo*E increase of about 0.05–0.08 MHz can be expected (or 0.01–0.02 MHz for the last 40 y). Also for this parameter the mean experimental trend value is slightly higher than the prediction. The observed *fo*E increase is also in qualitative agreement with trends of the ion ratio $[NO^+]/[O_2{}^+]$ obtained from mass spectrometer measurements by Danilov and Smirnova (1997). They found, for E region heights, a strong negative trend in $[NO^+]/[O_2{}^+]$ which causes a decreasing effective recombination coefficient (as the dissociative recombination coefficient of the NO^+ ions is about twice that of the $O_2{}^+$ ions) and therefore an increase of the electron density at the E region peak height. The negative trend in $[NO^+]/[O_2{}^+]$ again is caused by the reduced NO density as expected after model calculations for increasing atmospheric greenhouse gases (Roble and Dickinson, 1989; Chakrabarty, 1997; Beig and Mitra, 1997).

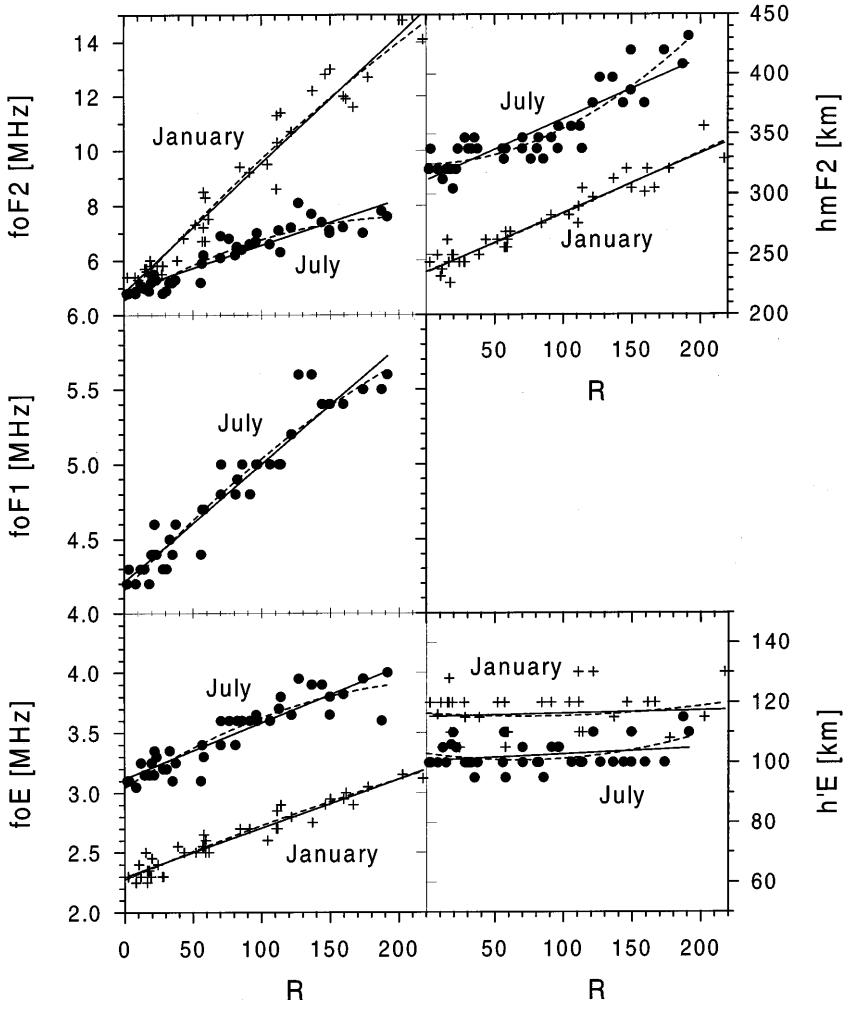

Fig. 7. Monthly median values of different ionosonde parameters of the station Juliusruh (12 LT, January and July, 1957–1996) in relationship to solar sunspot number R fitted by linear (*complete lines*) and quadratic curves (*dashed*)

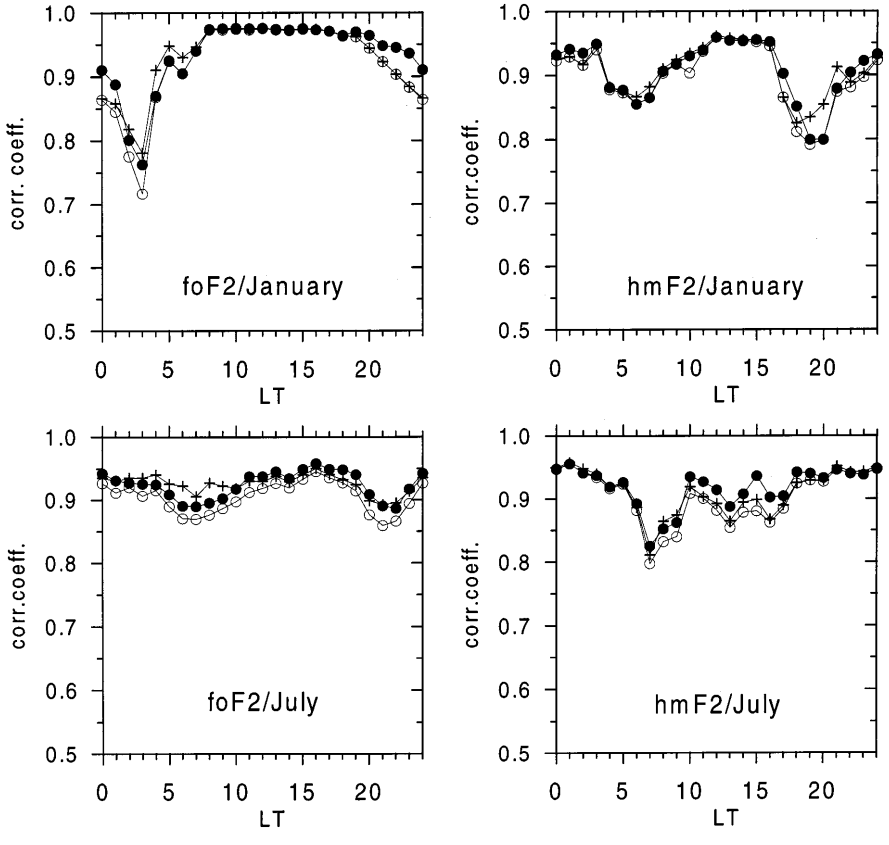

Fig. 8. Correlation coefficients between experimental monthly median *fo*F2 or *hm*F2 data (Juliusruh, January and July, 1957–1996) and different model values assuming a linear (*open circles*) or quadratic dependence on solar sunspot number R (*solid circles*) and for a twofold regression with R and geomagnetic Ap values (*crosses*) in dependence on local time LT

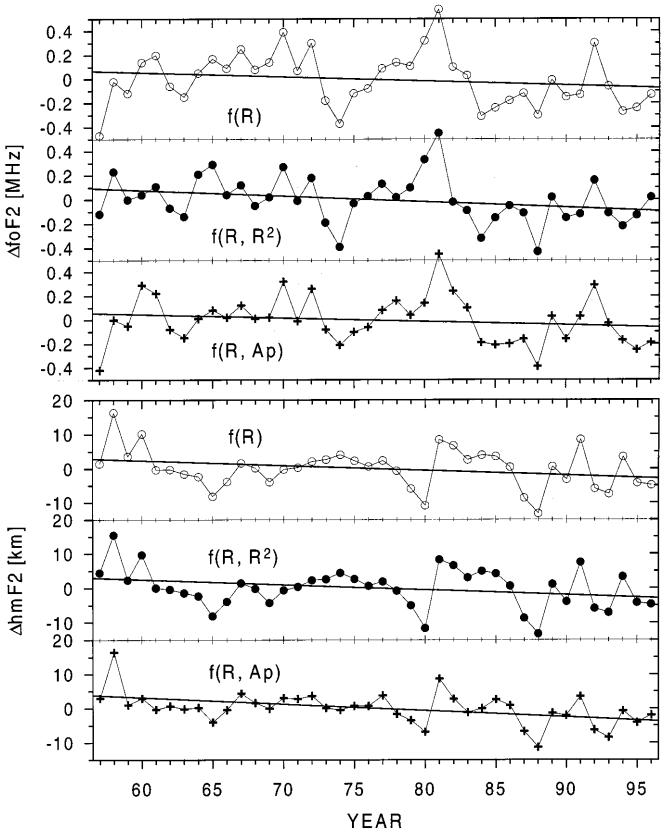

Fig. 9. Trends in *fo*F2 and *hm*F2 values of Juliusruh after removing the solar induced variation by a linear model $f(R)$, a quadratic model $f(R,R^2)$ and a twofold linear model $f(R, Ap)$ with the solar sunspot number and the geomagnetic *Ap* index

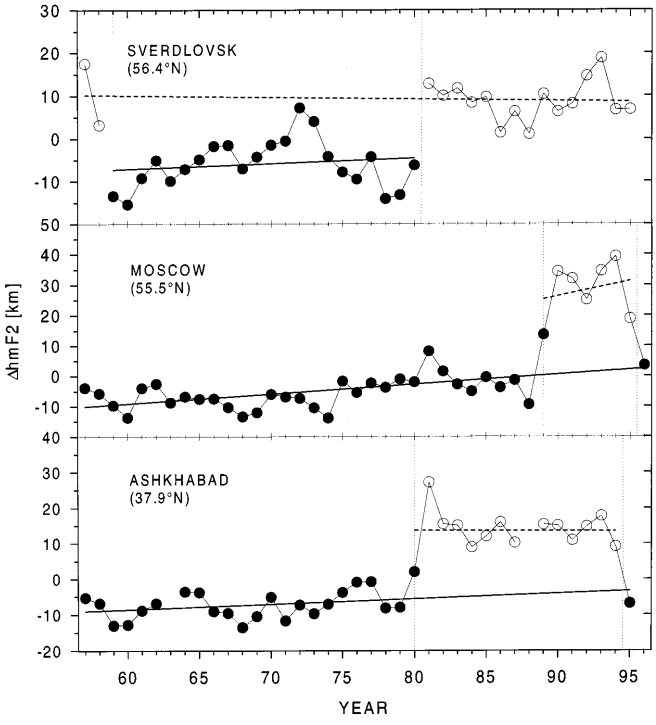

Fig. 10. Yearly trends of Δ*hm*F2 after elimination of the solar and geomagnetic influences for three stations with sudden Δ*hm*F2 changes (near the *dotted vertical lines*) which could be caused by technical changes

5 Conclusions

Based on observations at 31 European ionosonde stations over the last 40 y long-term trends have been derived at different ionospheric parameters of the E, F1 and F2 regions. In spite of marked differences between the results derived at single stations some common results could be found:

1. Technical changes of equipment or the evaluation algorithms used may partly influence the trend results derived for individual stations. However the comparison of the results of many different stations allows the derivation of representative (median) trends for the European region (5°W −70° E; 35°N - 70°N).
2. The trends in the E and F1 layers with lowering of the E region height, *h*′E, and increases of the peak electron densities, *fo*E and *fo*F1, do not depend on latitude and longitude and are in qualitative agreement with modelling results of the atmospheric greenhouse effect. The experimental mean trends are, however, stronger by a factor of 2..5 compared with the theoretical predictions for the E region and smaller by a factor of 2 with F1 region predictions.
3. The trends in the F2 region (*hm*F2 and *fo*F2) do not depend on latitude but show marked differences for the longitudinal regions west or east of 30° E. Whereas at longitudes west of 30° E the trends in *hm*F2 as well as *fo*F2 are in general negative as expected after model calculations for an atmospheric greenhouse effect, the trends in the European region east of 30° E are in general positive. These longitudinal differences are more pronounced in the *hm*F2 data but could also be detected in the *fo*F2 data. The cause of these regional differences which were also found by Ulich and Turunen (1997b) in world-wide *hm*F2 data is unknown at present and needs further investigations.

Acknowledgements. This work was partly supported by the Bundesministerium für Bildung, Wissenschaft, Forschung und Technologie (BMBF), Bonn, under contract 07VKV01/1.

Topical Editor D.Alcaydé thanks J. Lastovicka and T.J. Fuller - Rowell for their help in evaluating this paper.

References

Beig, G., and A. P. Mitra, Atmospheric and ionospheric response to trace gas perturbations through the ice age to the next century in the middle atmosphere. Part I - chemical composition and thermal structure, *J. Atmos. Solar-Terr. Phys.* **59,** 1245–1259, 1997.

Bilitza, D., N. M. Sheikh, and R. Eyrig, A global model for the height of the F2-peak using M3000 values from the CCIR numerical map, *Telecom J.*, **46,** 549–553, 1979.

Brasseur, G., and A. de Rudder, The potential impact on atmospheric ozone and temperature of increasing trace gas concentrations, *J. Geophys. Res.*, **92,** 10903–10920, 1987.

Bremer, J., Ionospheric trends in mid-latitudes as a possible indicator of the atmospheric greenhouse effect, *J. Atmos. Terr. Phys.,* **54,** 1505–1511, 1992.

Bremer. J., Some additional results of long-term trends in vertical-incidence ionosonde data, *Paper 4051, presented at the COST 251 Meeting, Prague,* 1996.

Bremer, J., Long-term trends in the meso- and thermosphere, *Adv. Space Res.,* **20,** (11), 2075–2083, 1997a.

Bremer, J., Long-term trends in the ionospheric E- and F- regions over Europe, *Paper 6306, presented at the COST 251 Meeting, Linköping,* 1997b.

Chakrabarty, D. K., Mesopause scenario on doubling of CO_2, *Adv. Space Res,* **20,** (11), 2117–2125, 1997.

Danilov, A. D., and N. V. Smirnova, Long-term trends in the ion composition in the E region (in Russian), *Geomagn. Aeron., 37,* (4), 35–40, 1997.

Houghton, J. T., L. G. Meira Filho, B. A. Callander, N. Harris, A. Kattenberg, and K. Maskell, *Climate Change 1995, Contribution of WGI to the Second Assessment Report of the Intergovernmental Panel on Climate Change,* Cambridge University Press, Cambridge, UK, 1996.

Kane, R. P., Solar cycle variation of foF2, *J.Atmos. Terr. Phys.* **54,** 1201–1205, 1992.

Kouris, S. S., P. A. Bradley, and I. K. Nissopoulos, The relationships for foF2 and M(3000)F2 versus R12, Numerical mapping and modelling and their application to PRIME, Scientific Report, *COST Document: COST238TD(94)010,* Eindhoven, 155–167, 1994.

Rishbeth, H., A greenhouse effect in the ionosphere?, *Planet. Space Sci.,* **38,** 945–948, 1990.

Rishbeth, H., and R. G. Roble, Cooling of the upper atmosphere by enhanced greenhouse gases – Modelling of thermospheric and ionospheric effects, *Planet. Space Sci.*, **40,** 1011–1026, 1992.

Roble, R. G., and R. E. Dickinson, How will changes in carbon dioxide and methane modify the mean structure of the mesosphere and thermosphere?, *Geophys. Res. Lett.*, **16,** 1441–1444, 1989.

Shimazaki, T., World wide daily variations in the height of the maximum electron density in the ionospheric F2 layer, *J. Radio Res. Labs., Japan*, **2,** 85–97, 1955.

Taubenheim, J., *Statistische Auswertung geophysikalischer und meteorologischer Daten,* Akad. Verlagsgesell. Geest and Portig K.-G., Leipzig, 1969.

Ulich, T. and E. Turunen, Evidence for long-term cooling of the upper atmosphere, *Geophys. Res. Lett.*, **24,** 1103–1106, 1997a.

Ulich, T., and E. Turunen, Long-term behavviour of ionospheric F2 layer peak height on a global scale, *Paper presented at Session 2.18 of the 8th Scientific Assembly of IAGA,* Uppsala, 1997b.